Mannosylated chitosan nanoparticle–based cytokine gene therapy suppressed cancer growth in BALB/c mice bearing CT-26 carcinoma cells

Tae Hee Kim,[1] Hua Jin,[2] Hyun Woo Kim,[2] Myung-Haing Cho,[2] and Chong Su Cho[1]

[1]Laboratory of Biomedical Polymer and Tissue Engineering, School of Agricultural Biotechnology and [2]Laboratory of Toxicology, College of Veterinary Medicine and BK21 Program for Veterinary Science, Seoul National University, Seoul, Korea

Abstract

Cancer immunotherapy relies on the ability of the immune system to destroy tumor cells selectively and to elicit a long-lasting memory of such activity. Interleukin-12 (IL-12) is an immunomodulatory cytokine produced primarily by antigen-presenting cells, which play an important role in promoting Th1-type immune response and cell-mediated immunity. To augment the antitumor immune action by *in vivo* IL-12 gene delivery, mannosylated chitosan (MC) was prepared to induce mannose receptor–mediated endocytosis of IL-12 gene directly into dendritic cells which reside within the tumor. Upon characterization, MC was proven to be suitable for IL-12 gene delivery due to good physicochemical properties and low cytotoxicity. In addition, MC exhibited much enhanced IL-12 gene transfer efficiency to dendritic cells rather than chitosan itself in terms of the induction of murine IL-12 p70 and murine IFN-γ. In animal studies, intratumoral injection of MC/plasmid encoding murine IL-12 complex into BALB/c mice bearing CT-26 carcinoma cells clearly suppressed tumor growth and angiogenesis, and significantly induced cell cycle arrest and apoptosis. Therefore, this study provides a new MC-mediated cytokine gene delivery system for cancer immunotherapy. [Mol Cancer Ther 2006;5(7): 1723–32]

Received 12/27/05; revised 4/17/06; accepted 5/17/06.

Grant support: Ministry of Science and Technology in Korea (M10414030002-05N1403-00210; T.H. Kim and C.S. Cho) and Nano Systems Institute-National Core Research Center (H. Jin, H.W. Kim, and M.H. Cho). H. Jin and H.W. Kim are recipients of a BK21 fellowship.

The costs of publication of this article were defrayed in part by the payment of page charges. This article must therefore be hereby marked advertisement in accordance with 18 U.S.C. Section 1734 solely to indicate this fact.

Note: T.H. Kim and H. Jin contributed equally to this work.

Requests for reprints: Chong Su Cho, Laboratory of Biomedical Polymer and Tissue Engineering, School of Agricultural Biotechnology, Seoul National University, Seoul 151-742, Korea. Phone: 82-2-880-4636; Fax: 82-2-875-2494. E-mail: chocs@plaza.snu.ac.kr or Myung-Haing Cho, Laboratory of Toxicology, College of Veterinary Medicine, Seoul National University, Seoul 151-742, Korea. Phone: 82-2-880-1276; Fax: 82-2-873-1268. E-mail: mchotox@snu.ac.kr

doi:10.1158/1535-7163.MCT-05-0540

Introduction

The aim of cytokine gene therapy for cancer lies in generating a long-lasting, tumor-specific, and systemic immune response for the prevention of tumor metastasis (1). Among the vast family of cytokines, interleukin-12 (IL-12) has proved to be one of the most effective inducers of potent antitumor immunity (2). IL-12 stimulates the proliferation of natural killer and T cells as well as augmenting their cytolytic activity, and induces the production of IFN-γ, and to a lesser extent, tumor necrosis factor-α, which enhances Th1-type immune response. Therefore, IL-12 is known to be able to suppress tumor progression, metastasis, and angiogenesis (3, 4).

IL-12 is produced primarily by professional antigen-presenting cells such as macrophages and dendritic cells, and exerts pleiotropic effects on immune effector cells (5, 6). In particular, dendritic cells are believed to play a critical role in antitumor immune responses because of their ability to stimulate cytotoxic T cells, which has been a major focus of vaccine and immunotherapeutic strategies for cancer therapy (7, 8). Other lines of evidence have reported that immature dendritic cells present in various kinds of tumors are unable to stimulate T cells because dendritic cells express low levels of costimulatory molecules and the majority of T cells infiltrating tumors have a naïve phenotype. The presence of naïve, but not memory or effector T cells, in tumors may be associated with the failure of tumoral dendritic cells to provide an adequate stimulus (9, 10). Therefore, local production of immunomodulatory cytokines such as IL-12 in tumor tissues may allow T cell activation and provide a critical clue to overcome a major barrier for successful immunotherapy.

Because stimulation of antitumor immune response by dendritic cells is critically dependent on their tightly regulated ability to produce IL-12, the enhancement of IL-12 production from dendritic cells is essential. Interestingly, immature dendritic cells express high levels of mannose receptors that are used for the endocytosis and phagocytosis of a variety of antigens. Following ligand binding, internalization, and release of cargo, mannose receptors are recycled and transported back to the cell surface where they allow repeated internalization of new ligand molecules (11). This finding prompted us to employ mannosylated cationic polymer for IL-12 gene delivery to the dendritic cells for effective cancer gene therapy.

Although ongoing gene therapy protocols mostly rely on viral vectors, nonviral gene transfer techniques have also gained increasing attention due to unique advantages such as less immune reaction against repeated administration, low cost, etc. Among various nonviral vectors, chitosan is considered to be a good candidate for gene delivery

because it is biocompatible, biodegradable, and has little toxic material with high cationic potential (12). Chitosan has also been reported to exhibit an immunostimulating activity, such as increasing the accumulation and activation of macrophages and polymorphonuclear cells, inducing cytokines, and cytotoxic T cell response (13). In this study, mannosylated chitosan (MC) was prepared to induce mannose receptor–mediated endocytosis of IL-12 gene directly into dendritic cells, which reside within the tumor, and to augment antitumor immune action via *in vivo* IL-12 gene delivery as a potent nanoparticle gene carrier for cancer immunotherapy.

Materials and Methods

Materials

Water-soluble chitosan (100 kDa; degree of deacetylation, 80%) was kindly donated by Prof. J.W. Nah (Sunchon National University, Korea), and the method of preparing the free amine water-soluble chitosan has been described previously (14). Anti-IL-12, anti-IFN-γ anti–proliferating cell nuclear antigen, anti-BAD, anti-BAX, anti-Bcl-xL, anti-p27, anti-p21, anti-p53, anti-cyclin D1, anti–cyclin-dependent kinase 4, anti–fibroblast growth factor-2 (FGF-2), and anti–vascular endothelial growth factor (VEGF) were purchased from Santa Cruz Biotechnology (Santa Cruz, CA). Anti-Apaf-1 was purchased from Upstate Biotechnology (Waltham, MA).

Plasmids

Plasmid encoding murine IL-12 (pmIL-12) was purchased from Aldevron (Fargo, ND). It was constructed using a cytomegalovirus immediate-early enhancer/promoter/intron-based plasmid with a kanamycin selection gene. The p35 and p40 subunits were separated by an internal ribosomal entry site and driven by a single cytomegalovirus promoter. pGL3 (~5.3 kb) containing SV40 promoter, resulting in strong expression of *luc*+, was purchased from Promega (Madison, WI). pEGFP-N2 (4.7 kb) encoding green fluorescent protein driven by an immediate-early promoter of cytomegalovirus was purchased from Clontech Laboratories (Palo Alto, CA).

Animals

ICR mice and BALB/c mice (6–8 weeks of age) were obtained from Jungang Lab Animal, Inc. (Seoul, Korea) and kept in our laboratory animal facility maintained at 23 ± 2°C, with a relative humidity of 50 ± 20%, and a 12-hour light/dark cycle. All methods used in this study were approved by the Animal Care and Use Committee at Seoul National University and conformed with the NIH guidelines (NIH publication No. 86-23, revised 1985).

Preparation of MC

Chitosan (60 mg) was dissolved in 1 mL of distilled water and mixed with mannopyranosylphenylisothiocyanate (Sigma-Aldrich, St. Louis, MO) in 1 mL of DMSO. The solution was stirred for 24 hours at room temperature. The polymer was precipitated by adding 10 volumes of isopropanol and spun down by centrifugation at 10,000 rpm for 20 minutes. The pellets were washed with isopropanol and collected by centrifugation at 10,000 rpm for 20 minutes. After repeating this process four times, pellets were dried in a vacuum oven. The composition of MC was determined by nuclear magnetic resonance spectroscopy (600 MHz; Bruker, Germany).

Preparation of MC/DNA Complex

MC/DNA charge ratio (N/P) was expressed as the ratio of moles of the amine groups of MC to those of the phosphate moieties of DNA. Complexes were induced to self-assemble in 10 mmol/L of phosphate buffer (pH 7.4) by mixing DNA plasmid with the appropriate polymer solution at the desired charge ratio. The complexes were allowed to stand at room temperature for 30 minutes. Complex formation was confirmed by electrophoresis on a 1% agarose gel with Tris-acetate running buffer at 100 V for 40 minutes. DNA was visualized with ethidium bromide (0.2 μg/mL). Protection of DNA in complexes was done via electrophoresis. MC/DNA complex and free DNA (pGL3; 0.2 μg) were separately incubated with DNase I (4 units) in DNase/Mg^{2+} digestion buffer [50 mmol/L of Tris-Cl (pH 7.6) and 10 mmol/L of $MgCl_2$] at 37°C and degradation of DNA was investigated by 1% agarose gel electrophoresis following incubation.

Atomic Force Microscopy

The morphology and sizes of MC/pGL3 complex were observed by Scanning Probe Microscope (Autoprobe CP, PSIA Inc., Fremont, CA). The complex solution prepared at charge ratio 5 was dropped on opposite charged mica and incubated for 2 minutes. Then, the mica was rinsed with distilled water, and dried at room temperature. Imaging was done using non–contact mode and V-shaped cantilevers with a pyramidal tip of silicon, the average complex sizes were determined by measuring the diameters of 50 complexes.

Cell Lines and Cell Culture

NCTC 3749 murine macrophage cells were incubated in RPMI 1640 (HyClone, Logan, UT), whereas Raw 264.7 murine macrophage cells and CT-26 murine colon adenocarcinoma cells were incubated in DMEM (Life Technologies, Paris, France) supplemented with 10% fetal bovine serum, streptomycin at 100 μg/mL, and penicillin at 100 units/mL. The cells were maintained at 37°C in a humidified 5% CO_2–containing atmosphere.

Preparation of Immature Dendritic Cells from Bone Marrow

Experiments were done with 6-week-old male ICR mice. After carefully removing all muscle tissue from the femurs and tibias of mice, the bones were placed in a 60 mm dish with 70% alcohol for 2 to 5 minutes, washed twice with PBS, and transferred onto a fresh dish with RPMI 1640. Then, both ends were cut with scissors and the marrow was flushed with RPMI 1640 using a syringe with a 26-gauge needle. Clusters within the marrow suspension were passed through a nylon mesh to remove small pieces of bone and debris, and red cells were lysed with ammonium chloride solution. To generate immature dendritic cells, the bone marrow cells were cultured with RPMI 1640 containing 10% heat-inactivated fetal bovine serum in the presence

of 20 ng/mL mouse granulocyte-macrophage colony–stimulating factor and 20 ng/mL mouse IL-4 (rmIL-4), and freshly prepared cytokines were added every other day. Dendritic cells were harvested at day 6.

Evaluation of Cytotoxicity

The cytotoxicity of chitosan and MC prepared at different concentrations of polymer were determined by using CellTiter 96 AQ_{ueous} One Solution Cell Proliferation Assay (Promega) following the manufacturer's protocol. The range of concentrations of polymer were determined by the amount applied to the transfection *in vitro* and *in vivo*. NCTC 3749 cells were seeded at a density of 4×10^4 cells/well in a 96-well plate, and incubated for 24 hours before being replaced by fresh serum-free RPMI 1640 containing chitosan and MC at various concentrations. Cells were incubated with polymers for 24 hours. Polymer-untreated cells in media were used as a control.

In vitro Transfection

For the luciferase assay, Raw 264.7 cells were seeded at a density of 3×10^5 cells in a 24-well plate, and cultured for 18 hours before transfection. Chitosan/DNA and MC/DNA complexes were prepared by mixing 1 μg of pGL3 with the appropriate amounts of chitosan or MC at charge ratio 5 and added to a 24-well plate and incubated for 4 hours. Serum-free media was replaced with growth media and incubated for another 48 hours at 37°C. The luciferase assay was done as previously described (15). For blocking experiments of MC/DNA transfection, Raw 264.7 cells were preincubated for 15 minutes with various concentrations of mannose, and transfection was done as described above. All the experiments were done in triplicate to ascertain reproducibility. In the case of the murine IL-12 (mIL-12) gene, dendritic cells were seeded at a density of 5×10^5 cells in a 24-well plate. Complexes were prepared by mixing 4 μg of pmIL-12 with the appropriate amounts of MC at a charge ratio of 5. The collected supernatants were analyzed for the measurement of mIL-12 p70 and murine IFN-γ using ELISA kits (R&D Systems, Minneapolis, MN).

Tumor Implantation and Treatment

To generate tumors, the back of 8-week-old male BALB/c mice (five animals/group) were shaved and 100 μL of single cell suspension containing 2×10^6 CT-26 cells were injected s.c. Tumor volume was calculated by using its mean diameter measured with vernier calipers and using the formula $v = 0.5 \times a \times b^2$, where a and b are the smallest and the largest diameters, respectively. Treatment of tumors was started after about 7 days when they reached a size of 100 to 120 mm^3. MC/pmIL-12 complexes were prepared at charge ratio 5 in normal saline and 100 μL of the complexes were injected directly into the tumors of BALB/c mice at a dose of 50 μg of DNA per mouse, at 3-day intervals for a total of four treatments (on days 0, 3, 6, and 9). MC/pcDNA3.1 complexes prepared under identical conditions were used as vector controls. CT-26 tumor-bearing mice treated with 100 μL of normal saline were used as a negative control. Tumor sizes were measured every 3 days. All the treated, vector control, and control mice were sacrificed on day 18, after which tumors were collected for further analysis. For *in vivo* GFP study, chitosan/pEGFP-N2 and MC/pEGFP-N2 complexes were prepared as described above, directly injected into the tumors of BALB/c mice at a dose of 50 μg DNA per mouse. Two days after injection, the mice were sacrificed, and the tumors were collected.

Western Blot Analysis

After measuring the protein concentration of the homogenized lysates using a Bradford kit (Bio-Rad, Hercules, CA), equal amounts (50 μg) of protein were separated on SDS-PAGE and transferred to nitrocellulose membranes. The membranes were blocked for 1 hour in TBS + Tween 20 containing 5% skimmed milk, immunoblotting was done by incubating the membranes overnight with their corresponding primary antibodies (1:1,000) at 4°C. Antibodies raised against IL-12, IFN-γ, BAD, BAX, BCL-XL, proliferating cell nuclear antigen, cyclin D1, cyclin-dependent kinase 4, VEGF, FGF-2, p53, p27, p21, and actin were purchased from Santa Cruz Biotechnology. Apaf-1 was purchased from Upstate Biotechnology. After washing in TBS + Tween 20, the membranes were incubated with horseradish peroxidase–labeled secondary antibodies (1:1,000). Antibodies raised against goat anti-rabbit IgG, goat anti-mouse IgG, and rabbit anti-goat IgG were purchased from Zymed (San Francisco, CA). The bands of interest were detected using a luminescent image analyzer, LAS3000 (Fujifilm, Japan). Results were quantified using Multi Gauge version 2.02 software (Fujifilm).

Terminal Deoxynucleotidyl Transferase–Mediated dUTP Nick End Labeling Assay

Formalin-fixed, paraffin-embedded tumor tissue slides were deparaffinized in xylene and rehydrated through alcohol gradient. The slides were washed with PBS, and nicked DNA ends were labeled by the terminal deoxynucleotidyl transferase–mediated dUTP nick end labeling method using an *in situ* cell death detection kit (Roche, Basel, Switzerland) following the manufacturer's protocol. As a final step, a tissue section was counterstained with methyl green (Trevigen, Gaithersburg, MD).

Gelatin Zymography Assay

The tumor tissues were homogenized and protein was measured using the Bradford kit (Bio-Rad). Equal amounts of protein were electrophoresed in 12% SDS-polyacrylamide gel containing 1% gelatin. The gel was then washed at room temperature for 2 hours with 2.5% Triton X-100 and subsequently incubated at 37°C in a buffer containing 10 mmol/L $CaCl_2$, 150 mmol/L NaCl, and 50 mmol/L Tris-HCl (pH 7.5) for 48 hours. The gel was then stained with Coomassie blue to visualize gelatinolytic activity.

Immunohistochemistry

Formalin-fixed, paraffin-embedded tissue sections were cut at 5 μm and transferred to plus slides (Fisher Scientific, Pittsburgh, PA). The tissues were deparaffinized in xylene and rehydrated through alcohol gradient. The tissue sections were incubated in 200 μL of proteinase K, and then washed and incubated in 3% hydrogen peroxide (AppliChem, Darmstadt, Germany) for 30 minutes to

quench endogenous peroxidase activity. After washing in PBS, the tissue sections were incubated with 3% bovine serum albumin in PBS for 1 hour at room temperature to block nonspecific binding sites. Primary antibody FGF-2 (1:100) was applied on tissue sections overnight at 4°C. The following day, the tissue sections were washed and incubated with secondary horseradish peroxidase–conjugated goat anti-rabbit IgG antibody (1:50) for 1 hour at room temperature. After careful washing, tissue sections were counterstained with Mayer's hematoxylin (DAKO, Carpinteria, CA) and washed with xylene. Coverslips were mounted using Permount (Fisher Scientific), and the slides were reviewed using a light microscope (Carl Zeiss, Thornwood, NY). For immunohistochemistry of CD11c, cryocut tumor sections (5 μm) were mounted on slides, air-dried, and stored desiccated at −80°C. Immediately before use, sections were fixed for 20 minutes in cold acetone, air-dried for 1 hour, and incubated in 0.3% hydrogen peroxide. Tumor sections were incubated with hamster anti-mouse CD11c Ab (BD PharMingen, San Diego, CA) followed by biotinylated anti-hamster cocktail (BD PharMingen) and streptoavidin-horseradish peroxidase (BD PharMingen) together with 3,3′-diaminobenzidine.

Data Analysis

Quantification of Western blot analysis was done using Multi Gauge version 2.02 software (Fujifilm). All results are given as the mean ± SE. Results were analyzed by Student's *t* test (GraphPad Software, San Diego, CA). *, $P < 0.05$ and #, $P < 0.05$ were considered significant and **, $P < 0.01$ and ##, $P < 0.01$ highly significant compared with the corresponding control and vector control, respectively.

Results

Characteristics of MC/DNA Complex

Nuclear magnetic resonance spectra revealed that synthesis of MC was completely successful and the substitution value of mannose was 7.3 mol % of total amine groups of chitosan. The DNA-carrying ability of MC was determined by gel retardation assays (Fig. 1A). The positively charged MC could make a strong complex with negatively charged phosphate moiety on the sugar backbone of DNA. When the charge ratio (N/P) reached 3, no free DNA was observed. In addition, MC successfully protected DNA plasmids from degradation by DNase I, and the MC/DNA complex at charge ratios of 5 to 20 were stable enough to carry the DNA (Fig. 1B). The morphology and sizes of MC/plasmid DNA complex prepared at charge ratio 5 were observed by atomic force microscopy (Fig. 1C). The atomic force microscopy image indicated that the complex was compacted and showed spherical or ellipsoidal structure with few aggregations. The average particle sizes of MC/plasmid DNA were 136.7 ± 33.5 nm. However, the aggregation pattern was increased as a function of charge ratios; thus, charge ratios of 10 or 20 could cause aggregation to some degree (data not shown). Based on the above findings, the MC/DNA complex prepared at charge ratio 5 was chosen for further *in vitro* and *in vivo* study. Figure 1D shows the cytotoxicity of chitosan and MC in NCTC 3749 macrophage cells over a wide range of concentrations. MC exhibited less toxicity than chitosan. Therefore, MC nanoparticles having low cytotoxicity as well as superior DNA-carrying capacity could be used as a suitable carrier for gene delivery.

In vitro Study

For initial studies, Raw 264.7 macrophage cells expressing moderate mannose receptors were used to determine

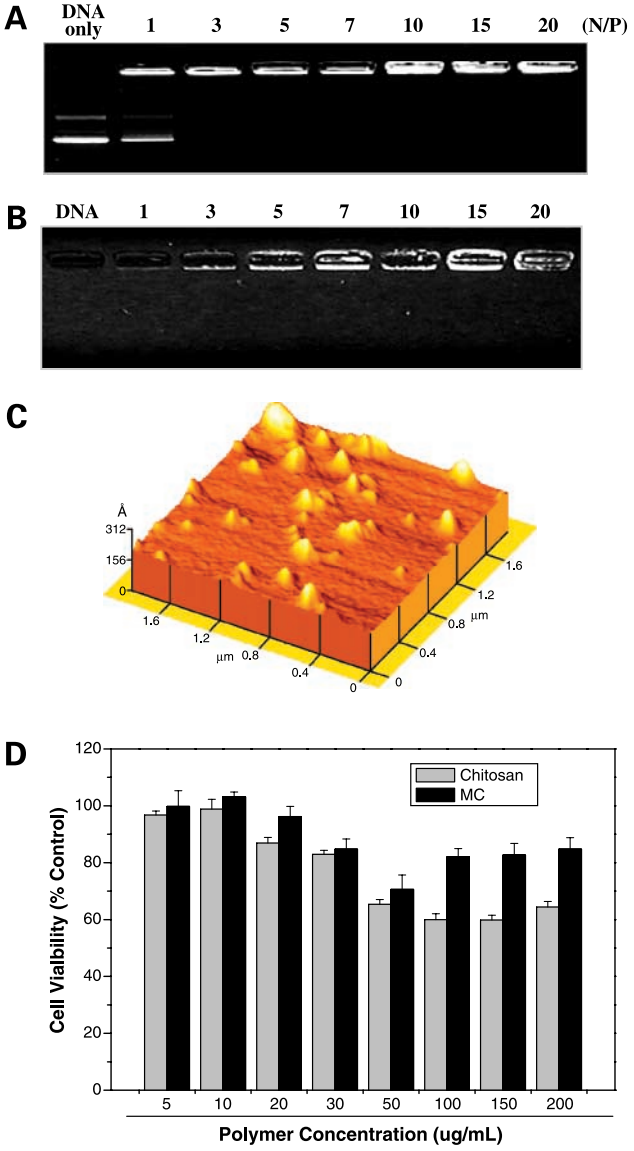

Figure 1. Characteristics of MC/DNA complex and cytotoxicity of MC. **A,** gel retardation assay of the MC/pGL3 complex. Charge ratio–dependent complex formation of MC/pGL3 was evaluated via agarose gel electrophoresis. Above charge ratio 3, the complex was stable enough to carry the DNA. **B,** DNase I protection assay. MC/pGL3 complex at the charge ratios of 5 to 30 showed high protection of DNA. **C,** representative atomic force microscopy image of MC/pGL3 complex at charge ratio 5. **D,** the cytotoxicity of chitosan and MC against NCTC 3749 macrophage cells. MC exhibited less toxicity than chitosan ($n = 5$; N/P, positive/negative).

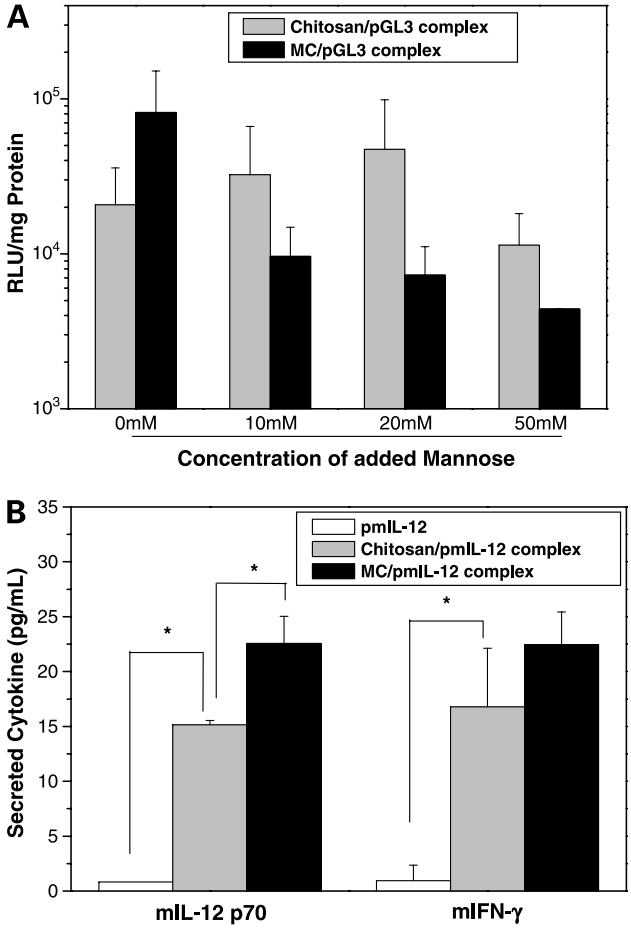

Figure 2. Mannose receptor–mediated DNA delivery and MC-induced cytokine secretion. **A,** mannose receptor–dependent DNA delivery in Raw 264.7 macrophage cells. The efficiency of DNA delivery in chitosan/pGL3 and MC/pGL3 complexes at charge ratio 5 was evaluated using luciferase assay. A distinctive mannose-dependent DNA delivery pattern was observed in MC/pGL3, but not in chitosan/pGL3, indicating that mannose receptor could moderate the MC-mediated DNA delivery (mean ± SD; $n = 3$). **B,** determination of mIL-12 p70 and mIFN-γ levels in dendritic cells. MC-mediated cytokine secretion was substantially higher than that of chitosan (mean ± SD; $n = 3$; RLU, relative light units; *, $P < 0.05$).

whether gene delivery with MC is mannose receptor–mediated. Our results clearly showed that MC-mediated pGL3 DNA transfection was mannose receptor–dependent because mannose could block the binding in a concentration-dependent manner. However, the complex of chitosan/pGL3 DNA did not show such a pattern (Fig. 2A). Our eventual goal was to apply the MC nanoparticle for cytokine gene delivery; thus, the efficiency of MC-mediated cytokine production was evaluated in dendritic cells collected from mice. As shown in Fig. 2B, the levels of mIL-12 p70, as well as murine IFN-γ, were significantly increased by MC/pmIL-12 and chitosan/pmIL-12 complexes compared with naked mIL-12. However, MC-mediated cytokine production was distinctively higher than that of chitosan. Based on the above findings, the MC/pmIL-12 complex was chosen for further *in vivo* study.

In vivo Study

To confirm whether MC is still a more efficient gene carrier for targeting dendritic cells *in vivo* compared with chitosan, GFP expression in tumors was observed using the MC/pEGFP-N2 and chitosan/pEGFP-N2 complexes, and dendritic cells were also immunohistochemically stained by anti-CD11c. As shown in Fig. 3A, MC induced much higher GFP expression than chitosan itself. The expression level of CD11c (visualized in dark brown color) was observed in a broad area of tumor tissues, indicating that dendritic cells reside widely within tumors. These results suggest that MC is a more efficient gene carrier for targeting dendritic cells *in vivo* compared with chitosan.

To examine the efficiency of IL-12 gene delivery using MC, the expressions of mIL-12 and murine IFN-γ were investigated by Western blotting. The MC/pmIL-12 complex prepared at charge ratio 5 was treated in BALB/c mice bearing CT-26 carcinoma cells. As shown in Fig. 3B and C, IL-12 expression by MC/pmIL-12 complex was significantly higher than control and vector control. The production of murine IFN-γ was also determined, because IL-12 primarily exerts its antitumor effect via indirect interaction with tumor cells by stimulating potent cytokines such as IFN-γ (16). The MC/pmIL-12 complex increased murine IFN-γ production significantly compared with control and vector controls as well. To investigate the relation between tumor growth and production of cytokines, tumor volume was measured twice a week after the treatment of the MC/pmIL-12 complex. Because some of the mice in vector control and control groups were dead, it was impossible to compare the tumor volume between control and treated groups after 12 days. The administration of MC/pmIL-12 complex suppressed *in vivo* tumor growth compared with control and vector control (Fig. 3D). Because there was no significant difference between the control and vector control in cytokine production and tumor size, the treated group with the MC/pmIL-12 complex was only compared with the control group for further studies.

Detection of Apoptosis

Apoptosis is an active process of cell death that occurs in response to a variety of agents including anticancer drugs. It involves balanced transcription of antiapoptotic genes such as Bcl-xL and proapoptotic genes such as Bad and Bax. Proapoptotic family members initiate apoptosis by inducing the release of cytochrome *c*, and cell death signals from mitochondria are coupled to downstream effector pathways through Apaf-1 (17). To investigate changes in the protein expression of Bad, Bax, Bcl-xL, and Apaf-1, tumor tissues treated with MC/pmIL-12 complex were analyzed by Western blotting. As shown in Fig. 4A and B, the expression levels of proapoptotic Bad, Bax, and Apaf-1 in treated groups were highly increased compared with control groups. In contrast, MC/pmIL-12 gene delivery caused a significant reduction of antiapoptotic Bcl-xL. To confirm the Western blot analysis,

terminal deoxynucleotidyl transferase–mediated dUTP nick end labeling assay was done. The results revealed that distinctive apoptotic processes were under way in the treated group compared with the control group, as confirmed by the presence of fragmented DNA, a direct evidence of apoptotic cell death (Fig. 4C). Our results strongly suggest that MC/pmIL-12 complex facilitates apoptosis in tumor tissues.

Regulation of Cell Cycle

To determine whether intratumoral injection of the MC/pmIL-12 complex was attributable to cell cycle arrest of tumor tissues, the expression of cell cycle–regulatory molecules was examined by Western blot. As shown in Fig. 5A and B, the expression of early G_1 marker, cyclin D1, cyclin-dependent kinase 4, and proliferating cell nuclear antigens were significantly down-regulated in the treated group. However, administration of MC/pmIL-12 caused a significant increase of representative G_1-S checkpoint molecules such as p21, and p27. In addition, the expression levels of p53 tumor suppressor genes were highly increased in treated mice.

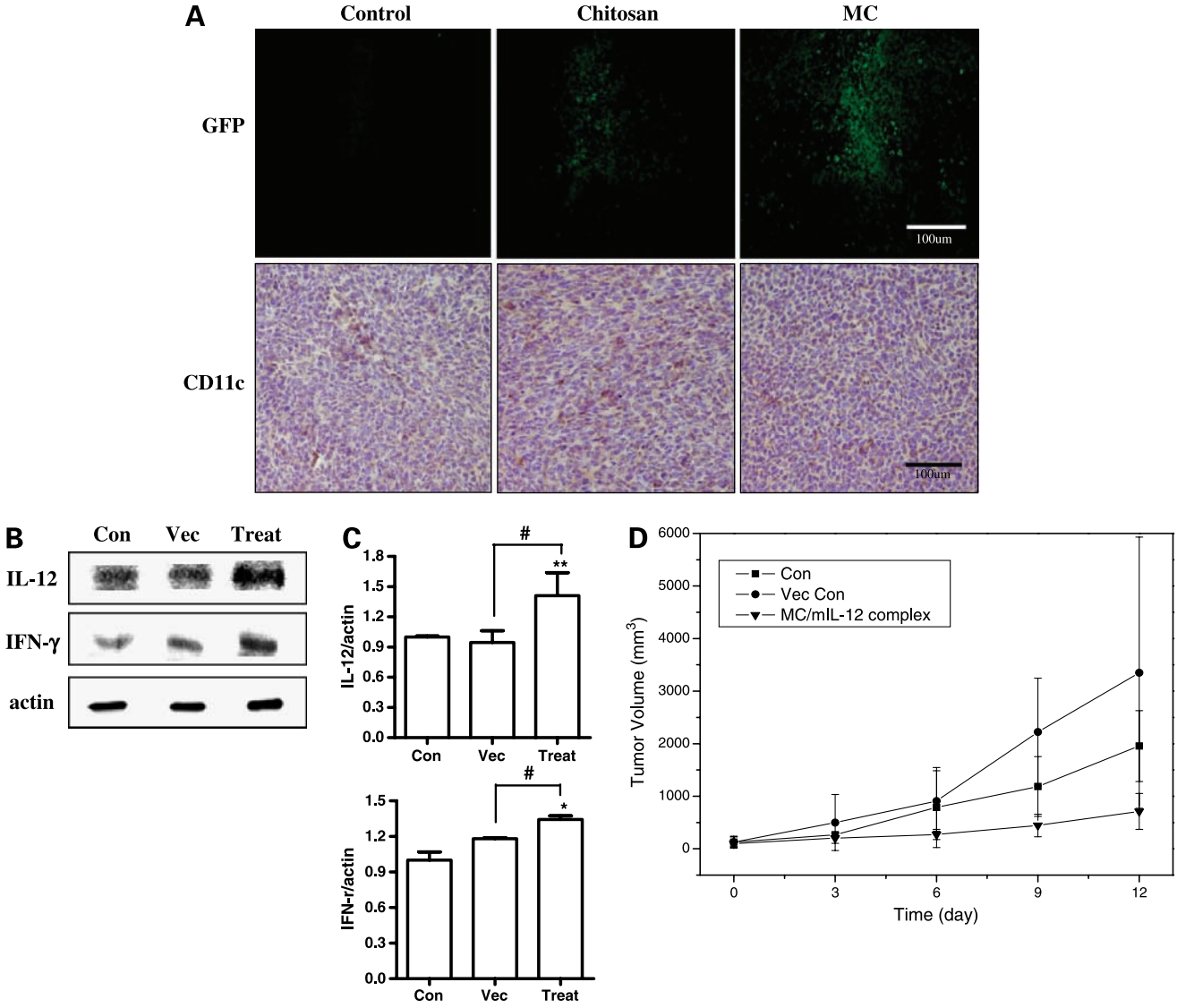

Figure 3. Effect of MC/pmIL-12 complex on tumor growth. **A,** delivery efficiency of chitosan and MC using chitosan/pEGFP-N2 and MC/pEGFP-N2 complex *in vivo*. Dendritic cells residing within tumor tissue were immunohistochemically stained by mouse anti-CD11c and visualized in dark brown color (original magnification, ×200). **B,** Western blot analysis of mIL-12 p70 and mIFN-γ in tumor tissues of BALB/c mice bearing CT-26 carcinoma cells treated with MC/pmIL-12. **C,** densitometric analysis of mIL-12 p70 and mIFN-γ. MC/pmIL-12 increased the level of mIL-12 p70 and mIFN-γ significantly compared with control and vector control (*, $P < 0.05$; **, $P < 0.01$ compared with control; #, $P < 0.05$ compared with vector control; $n = 5$). **D,** suppression of tumor growth by MC/pmIL-12. The tumor volume in BALB/c mice bearing CT-26 carcinoma cells was recorded every 3 d. MC/pmIL-12 complex suppressed the tumor growth effectively.

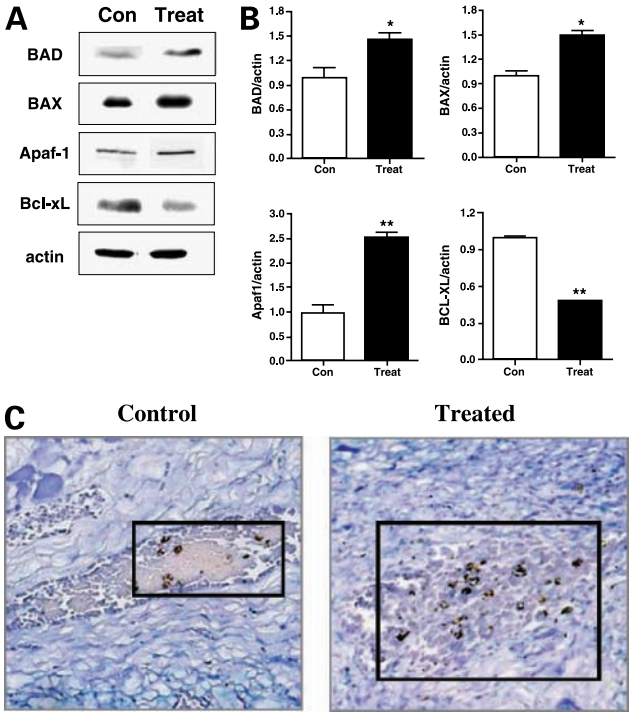

Figure 4. Induction of apoptosis by MC/pmIL-12 complex. **A,** Western blot analysis of apoptosis-related proteins. MC/pmIL-12 complex increased the protein expression of proapoptotic signals such as Bad, Bax, and Apaf-1, but decreased the level of antiapoptotic Bcl-xL. **B,** densitometric analysis of apoptosis-related protein expressions. Data were normalized to actin (**, $P < 0.01$, compared with control; $n = 3$). **C,** terminal deoxynucleotidyl transferase–mediated nick end labeling assay. Apoptotic signals (*dark brown color*) were clearly detected in tumor tissues from animals treated with MC/pmIL-12 complex compared with control (original magnification, ×200).

Inhibition of Angiogenesis

Matrix metalloproteinases, especially matrix metalloproteinase-2, are known to be actively involved in tumor angiogenesis, tumor growth, and metastasis mainly through their degradative capacity (18). To examine the potential effect of MC/mIL-12 complex on matrix metalloproteinase-2 activities in tumor tissue, zymography assays were done. As expected, strong inhibitory activity against MMP-2 was observed in the treated group (Fig. 6A). Also, FGF-2 and VEGF are important stimulators of angiogenesis which have been implicated in neoplastic progression (19). To test whether the MC/pmIL-12 complex affects the protein expression level of FGF-2 and VEGF, Western blot and immunohistochemistry were done. As shown in Fig. 6B and C, MC/pmIL-12 gene delivery caused a significant reduction of FGF-2 and VEGF. Furthermore, the expression level of FGF-2 (visualized in dark brown color) was decreased significantly in the treated group compared with the controls, which had a similar pattern to zymography and Western blot results (Fig. 6D). These results suggest that the administration of MC/pmIL-12 complex effectively leads to the abrogation of tumor angiogenesis and growth.

Discussion

Cancer cells evade host immune surveillance due to their low immunogenicity, reduced or absent expression of MHC class I, TAP-1, TAP-2, or costimulatory molecules (20). Strategies to augment the host immune response against cancer cells include vaccinations by gene-modified tumor cells or pulsing antigen-presenting cells with tumor-associated antigens. Recent studies have shown that vaccination of tumor cells fused with antigen-presenting cells such as dendritic cells or B cells could effectively elicit a host T cell–mediated antitumor response (21). Furthermore, the administration of immunomodulatory cytokines could be another important strategy for generating and enhancing immune response against cancer. A variety of strategies have been devised to use dendritic cells to stimulate immunity, and most of these strategies rely on the activation and maturation of dendritic cells *ex vivo* (5, 20, 21). However, *ex vivo* manipulation of dendritic cells is time-consuming and costly, requires the use of numerous cytokines, and

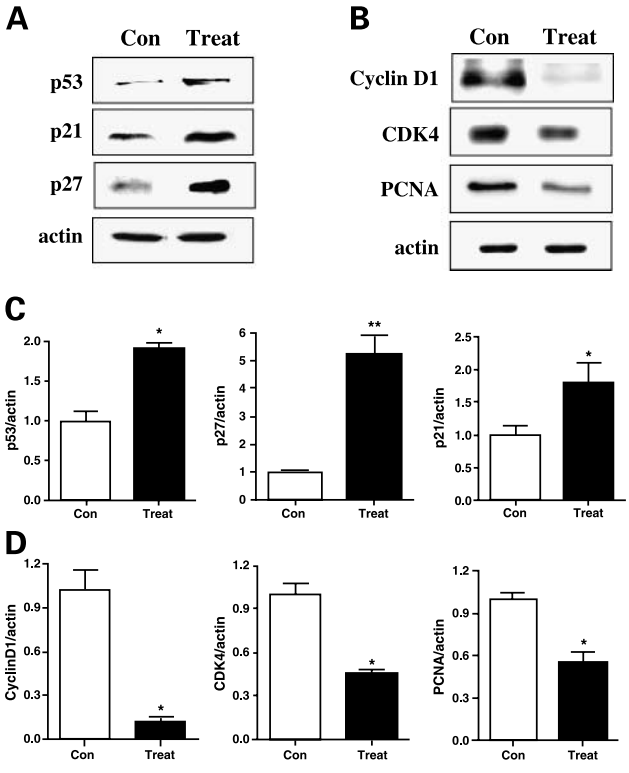

Figure 5. Western blot analysis of cell cycle signaling proteins. **A,** tumor tissues from control and treated mice were analyzed for protein levels of p21, p27, and p53 by Western blot. **B,** Western blot analysis of protein levels of cyclin D1, CDK4, and proliferating cell nuclear antigen. **C,** densitometric analysis of cell cycle proteins. Data were normalized to actin (*, $P < 0.05$; **, $P < 0.01$, compared with control; $n = 3$). MC/pmIL-12 complex suppressed proliferating cell nuclear antigen, cyclin D1, and CDK4, representative early G_1-S cell cycle checkpoint. However, MC/pmIL-12 complex increased cell cycle inhibitors such as p21 and p27. The complex also increased protein expression of tumor suppressor gene p53.

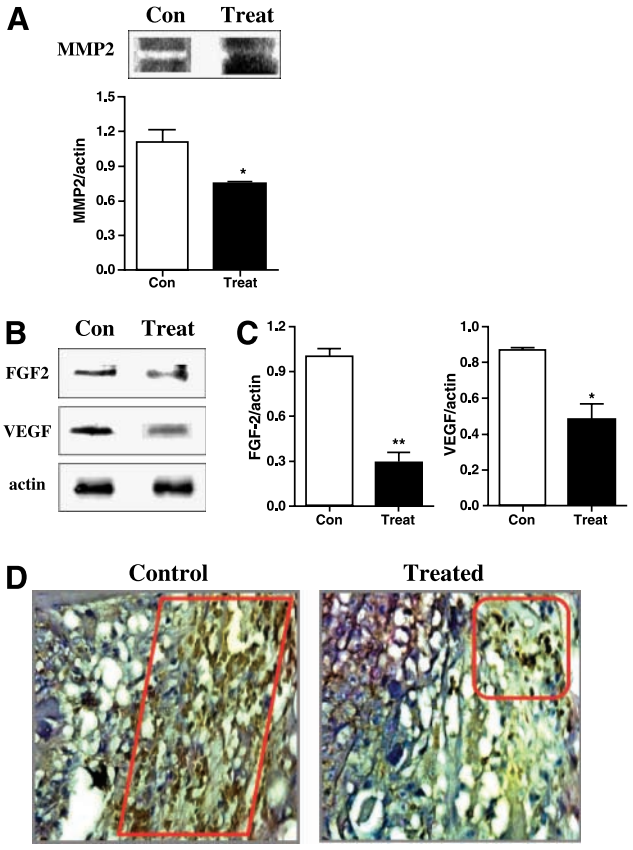

Figure 6. Effect of MC/pmIL-12 complex on tumor angiogenesis. **A,** gelatin zymography assay for the activity of matrix metalloproteinase-2. **B,** Western blot analysis of FGF-2 and VEGF. **C,** densitometric analysis of angiogenesis proteins. Data were normalized to actin (*, $P < 0.05$; **, $P < 0.01$, compared with control; $n = 3$). MC/pmIL-12 complex suppressed FGF-2 and VEGF significantly. **D,** immunohistochemical analysis of FGF-2. Positive signals were visualized in dark brown color. The expression of FGF-2 was substantially reduced in mice treated with the MC/pmIL-12 complex compared with controls (original magnification, ×200).

exposes the patient to the risk of infection. In the present study, we attempted to increase the immune response by delivering the IL-12 gene, directly targeting dendritic cells which reside within the tumor tissue.

MC nanoparticles were prepared as IL-12 gene carriers to induce mannose receptor–mediated endocytosis into dendritic cells. MC successfully condensed and protected DNA plasmids from degradation by nucleases (Fig. 1). MC/DNA complex prepared at charge ratio 5 proved to be the optimal condition for minimal aggregation, and the particle sizes were in the range of 103 to 170 nm. Low aggregate formation and small sizes of MC/DNA complex with low cytotoxicity would facilitate the delivery efficiency. Such characteristics may be explained by steric hindrance and the charge shielding effect of mannose in MCs. Recent evidence suggests that the introduction of sugar in polycations affects electrostatic interactions between anionic cell surfaces and cationic polymer, and thereby reduces membrane-damaging effects typical for polycations (22). Therefore, nanosized MCs are expected to be suitable carriers for gene therapy because of their good physicochemical properties and low cytotoxicity.

Macrophages and dendritic cells have substantial amounts of mannose receptors on the surface, suggesting that MC-mediated gene delivery may be induced by receptor-mediated endocytosis via surface-bound mannose receptors. Our results can be further confirmed by the finding that mannosylated polyethylenimine was more effective for gene expression in dendritic cells than unconjugated polyethylenimine, and that mannosylated bovine serum albumin blocked the uptake of mannosylated polyethylenimine/DNA complexes (23). Kawakami et al. also reported that the mannose receptor–mediated pathway was effective for gene expression in macrophages (24). In fact, the MC/DNA complex was more efficient for transferring IL-12 gene into dendritic cells than the chitosan/DNA complex, resulting in better induction of IFN-γ and mIL-12 p70 from dendritic cells (Fig. 2).

As expected from the *in vitro* study results, MC proved to be a more efficient gene carrier for targeting dendritic cells *in vivo* compared with chitosan itself. Furthermore, intratumoral delivery of the MC/pmIL-12 complex into BALB/c mice bearing CT-26 tumor cells resulted in high expression levels of IL-12 p70 and IFN-γ, suggesting that tumor growth was retarded due to the higher production of both cytokines compared with controls (Fig. 3). Our results are supported by previous findings that the immunomodulatory activities of IL-12 p70 induced IFN-γ to regulate the function of tumor-infiltrating immune cells such as T cells, natural killer cells, and macrophages, leading to retardation or even significant regression of tumor growth after treatment with IL-12 (25, 26).

Our findings showed that such a strong antitumor activity of the MC/pmIL-12 complex was closely associated with apoptosis, cell cycle arrest, and antiangiogenesis. Our results are supported by the findings that the therapy of attenuated *Salmonella typhimurium* vaccine strain encoding murine VEGF combined with the IL-12 gene has a significant effect against tumors by facilitating apoptosis (27). As mentioned earlier, the induction of cell cycle arrest was found to be related with the apoptosis of tumor tissue in our study. These results are supported by the findings that apoptosis and the cell cycle share some common participants—including Rb, E2F, and p53—and exhibit morphologic similarities of cell rounding and chromatin condensation, suggesting that both processes might be regulated to some extent by similar molecular mechanisms (28). The function of cyclin-dependent kinase activity is tightly regulated by cell cycle inhibitors such as the p21 and p27 Cip/Kip proteins (29). In addition, the p53 tumor suppressor protein is an important regulator of p21 and is a direct inducer of cell death by stimulating the expression of proapoptotic genes including Bax and Apaf-1 (30). Our results are supported by the findings that IFN-γ induced the accumulation of

p53 and p21 in the human squamous carcinoma cell line, ME180S (31). Taken together, these findings indicate that the IL-12 expressed from the MC/pmIL-12 complex and IFN-γ induced by IL-12 induce apoptosis and cell cycle arrest in tumor tissue.

Angiogenesis is known to be a prerequisite for tumor growth, because tumors cannot grow beyond several cubic millimeters when new vessel formation is blocked (32). Treatment with MC/pmIL-12 complex showed the effect of antiangiogenesis by losing the activities of matrix metalloproteinase-2, VEGF, and FGF-2 (Fig. 6), which are the beginning steps of tumor angiogenesis. Dendritic cells are very efficient at internalizing apoptotic bodies and taking up antigens from compartments of the tumor nodule undergoing programmed cell death (33). Therefore, secreted IL-12 by intratumoral administration of MC/pmIL-12 complex into the tumor site may down-regulate angiogenesis or mediate other antitumor effects. Our findings are supported by several previous reports. Recent evidence indicates that IL-12 exerts autocrine function on dendritic cell maturation as well as migration through the activation of nuclear factor κB transcription factors (34). In addition, several studies have shown that IL-12 could mediate antitumor functions partly through IFN-γ (26, 35). In conjunction with IFN-γ, IL-12 induces the differentiation of a T helper 1 immune response, which may promote the establishment of an antitumor immune response through increased IFN-γ production or by conditioning dendritic cells to activate antigen-specific $CD8^+$ T cells (36).

In conclusion, MC nanoparticles were successfully prepared and their potential as an *in vivo* targeting gene delivery system was evaluated. We have shown that MC/pmIL-12 complexes could inhibit tumor growth through diverse functions such as antiangiogenesis, induction of cell cycle arrest, and apoptosis. We also propose that biocompatible MC nanoparticles are fit for repeated administration to maintain sustained gene expression, thereby opening the possibility for novel cancer immunotherapy.

References

1. Mendiratta SK, Quezada A, Matar M, et al. Intratumoral delivery of IL-12 gene by polyvinyl polymeric vector system to murine renal and colon carcinoma results in potent antitumor immunity. Gene Ther 1999;6:833 – 9.

2. Harada M, Tamada K, Abe K, Yasumoto K, Kimura G, Nomoto K. Role of the endogenous production of interleukin 12 in immunotherapy. Cancer Res 1998;58:3073 – 7.

3. Maheshwari A, Han S, Mahato RI, Kim SW. Biodegradable polymer-based interleukin-12 gene delivery: role of induced cytokines, tumor infiltrating cells and nitric oxide in antitumor activity. Gene Ther 2002;9: 1075 – 84.

4. Pham-Nguyen KB, Yang W, Saxena R, Thung SN, Woo SL, Chen SH. Role of NK and T cells in IL-12-induced anti-tumor response against hepatic colon carcinoma. Int J Cancer 1999;81:813 – 9.

5. Shimizu T, Berhanu A, Redlinger RE, Watkins S, Lotze MT, Barksdale EM. Interleukin-12 transduced dendritic cells induce regression of established murine neuroblastoma. J Pediatr Surg 2001;36: 1285 – 92.

6. Lamont AG, Adorini L. IL-12: a key cytokine in immune regulation. Immunol Today 1996;17:214 – 7.

7. Furumoto K, Mori A, Yamasaki S, et al. Interleukin-12-gene transduction makes DCs from tumor-bearing mice an effective inducer of tumor-specific immunity in a peritoneal dissemination model. Immunol Lett 2002; 83:13 – 20.

8. Banchereau J, Steinman RM. Dendritic cells and the control of immunity. Nature 1998;392:245 – 52.

9. Furumoto K, Soares L, Engleman EG, Merad M. Induction of potent antitumor immunity by *in situ* targeting of intratumoral DCs. J Clin Invest 2004;113:774 – 83.

10. Vicari AP, Caux C, Trinchieri G. Tumor escape from immune surveillance through dendritic cell inactivation. Semin Cancer Biol 2002; 12:33 – 42.

11. Egan BS, Abdolrasulnia R, Shepherd VL. IL-4 modulates transcriptional control of the mannose receptor in mouse FSDC dendritic cells. Arch Biochem Biophys 2004;428:119 – 30.

12. Bozkir A, Saka OM. Chitosan-DNA nanoparticles: effect on DNA integrity, bacterial transformation and transfection efficiency. J Drug Target 2004;12:281 – 8.

13. Seferian PG, Martinez ML. Immune stimulating activity of two new chitosan containing adjuvant formulation. Vaccine 2001;19:661 – 8.

14. Jang MK, Jeong YI, Cho CS, Yang SH, Kang YE, Nah JW. The preparation and characterization of low molecular and water soluble free-amine chitosan. Bull Korean Chem Soc 2002;23:914 – 6.

15. Kim TH, Park IK, Nah JW, Choi YJ, Cho CS. Galactosylated chitosan/DNA nanoparticles prepared using water-soluble chitosan as gene carrier. Biomaterials 2004;25:3783 – 92.

16. Haicheur N, Escudier B, Dorval T, et al. Cytokines and soluble cytokine receptor induction after IL-12 administration in cancer patients. Clin Exp Immunol 2000;119:28 – 37.

17. Adams JM, Cory S. Apoptosomes: engines for caspase activation. Curr Opin Cell Biol 2002;14:715 – 20.

18. Klein G, Vellenga E, Fraaije MW, Kamps WA, de Bont ES. The possible role of matrix metalloproteinase (MMP)-2 and MMP-9 in cancer, e.g. acute leukemia. Crit Rev Oncol Hematol 2004;50:87 – 100.

19. Plum SM, Holaday JW, Ruiz A, Madsen JW, Fogler WE, Fortier AH. Administration of a liposomal FGF-2 peptide vaccine leads to abrogation of FGF-2-mediated angiogenesis and tumor development. Vaccine 2000;19: 1294 – 303.

20. Nishioka Y, Hirao M, Robbins PD, Lotze MT, Hideaki T. Induction of systemic and therapeutic antitumor immunity using intratumoral injection of dendritic cells genetically modified to express interleukin 12. Cancer Res 1999;59:4035 – 41.

21. Alli RS, Khar A. Interleukin-12 secreted by mature dendritic cells mediates activation of NK cell function. FEBS Lett 2004;559:71 – 6.

22. Kunath K, von Harpe A, Fischer D, Kissel T. Galactose-PEI-DNA complexes for targeted gene delivery: degree of substitution affects complex size and transfection efficiency. J Control Release 2003;88: 159 – 72.

23. Diebold SS, Kursa M, Wagner E, Cotton M, Zenke M. Mannose polyethylenimine conjugates for targeted DNA delivery into dendritic cells. J Biol Chem 1999;274:19087 – 94.

24. Kawakami S, Sato A, Nishikawa M, Yamashita F, Hashida M. Mannose receptor-mediated gene transfer into macrophages using novel mannosylated cationic liposomes. Gene Ther 2000;7: 292 – 9.

25. Brunda MJ, Luistro L, Warrier RR, et al. Antitumor and antimetastatic activity of interleukin-12 against murine tumors. J Exp Med 1993;178: 1223 – 30.

26. Nastala CL, Edington HD, Mckinney TG, et al. Recombinant IL-12 administration induces tumor regression in association with IFN-γ production. J Immunol 1994;153:1697 – 706.

27. Keke F, Hongyang Z, Hui Q, Jixiao L, Jian C. A combination of flk 1-based DNA vaccine and immunomodulatory gene (IL-12) in the treatment of murine cancer. Cancer Biother Radiopharm 2004;19: 649 – 57.

28. King KL, Cidlowski JA. Cell cycle and apoptosis: common pathways to life and death. J Cell Biochem 1995;58:175 – 80.

29. Coqueret O. New roles for p21 and p27 cell-cycle inhibitor: a function for each cell compartment? Trends Cell Biol 2003;13:65 – 70.

30. Fortin A, Cregan SP, MacLaurin JG, et al. APAF1 is a key

transcriptional target for p53 in the regulation of neuronal cell death. J Cell Biol 2001;155:207–16.

31. Akca H, Ozes ON. Epidermal growth factor suppresses interferon-induced accumulation of p53 and p21 by using protein kinase C. Scand J Clin Lab Invest 2003;63:505–12.

32. Folkman J. Tumor angiogenesis. In: Mendelsohn J, Howley PM, Israel MA, Liotta LA, editors. The molecular basis of cancer. Philadelphia: Saunders; 1995. p. 206–32.

33. Albert ML, Sauter B, Bhardwaj N. Dendritic cells acquire antigen from apoptotic cells and induce class I-restricted CTLs. Nature 1998;392:86–9.

34. Grohmann U, Belladonna ML, Bianchi R, et al. IL-12 acts directly on DC to promote nuclear localization of NF-κB and primes DC for IL-12 production. Immunity 1998;9:315–23.

35. Brunda MJ, Luistro L, Hendrzak JA, Fountoulakis M, Garotta G, Gately MK. Role of interferon-γ in mediating the antitumor efficacy of interleukin-12. J Immunother Emphasis Tumor Immunol 1995;17:71–7.

36. Ridge JP, Di Rosa F, Matzinger P. A conditioned dendritic cell can be a temporal bridge between a CD4+ T-helper and a T-killer cell. Nature 1998;393:474–8.